I&EC research
Industrial & Engineering Chemistry Research

pubs.acs.org/IECR

Article

Investigating the Impact of Synthesis Conditions to Increase the Yield and Tin Incorporation Efficiency for Lewis Acid Nano-Sn-MFI Zeolites

Medha Kasula, Alexander P. Spanos, Leah Ford, and Nicholas A. Brunelli*

Cite This: *Ind. Eng. Chem. Res.* 2022, 61, 1977−1984

Read Online

ACCESS | Metrics & More | Article Recommendations | Supporting Information

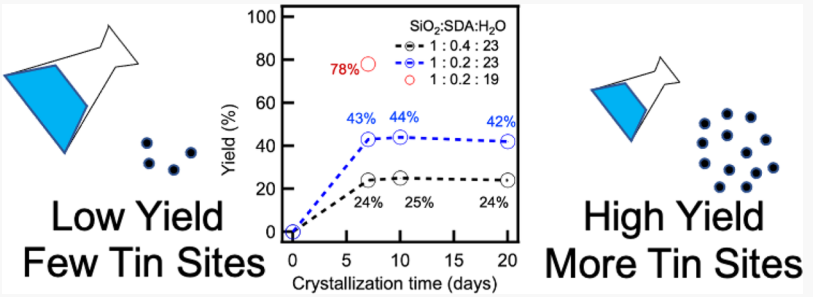

ABSTRACT: Advances in the synthesis of Lewis acid zeolites have been bolstered by the synthesis of nano-zeolites to overcome diffusion limitations. Key challenges remain for the synthesis of Lewis acid nano-zeolites since current methods tend to result in a low tin incorporation efficiency (25%) and a low material yield (~25%). In this work, insights on how to overcome these limitations are investigated through synthesizing nano-zeolite MFI with different tin precursors (n-Sn-MFI) and different ratios of water to silica and/or structure directing agent (SDA) to silica. The crystallization process is monitored using dynamic light scattering, and it is determined that the tin precursor has a minor impact on the final particle size, but the water and SDA concentrations did affect the final particle size. Compared to the standard synthesis (SiO_2/SDA/H_2O of 1:0.4:23), reducing the amount of SDA/SiO_2 to 0.2:1 results in a larger particle size but increases the yield and tin incorporation efficiency. Reducing the amount of water (H_2O/SiO_2 of 19 and SDA/Si of 0.2) improves the tin incorporation efficiency over the standard case and results in small particles while achieving a yield of up to 78%. The resulting materials are characterized using several standard techniques to demonstrate that the materials are of high quality. The materials are tested for catalytic activity in the alcohol ring opening reaction of epoxide as a probe reaction and are found to have comparable activity. The rate of conversion of 1,2-epoxyhexane can be increased through synthesizing small crystals in high yield through decreasing the SDA/SiO_2 ratio to 0.2:1 and reducing the H_2O/SiO_2 ratio to 19:1. Overall, the work demonstrates that the synthesis conditions can be tuned to increase the tin incorporation efficiency and increase the yield of the Lewis acid nano-zeolites while producing a highly active catalyst.

INTRODUCTION

The synthesis of Lewis acid zeolites has opened up a new domain of chemical transformations for heterogeneous catalytic materials. Indeed, Lewis acid zeolites have been used to catalyze many important reactions.[1−10] As the application space expands for Lewis acid zeolites, it becomes useful to expand the scope of potential substrates. However, large substrates tend to encounter diffusion limitations in the small pores of zeolites.[11−13] These diffusion limitations can be mitigated through reducing the overall dimensions of the materials to the nanoscale. Whereas the synthesis of pure silica and aluminosilicate nano-zeolites has been investigated extensively,[14−16] the synthesis of Lewis acid nano-zeolites has received limited attention.[9,17,18] The potential of Lewis acid nano-zeolites would benefit from further investigating the range of potential synthetic conditions that can be used to produce highly active catalytic materials.

The synthesis of zeolites with nanoscale dimensions has been achieved through different methods, including through controlling the particle morphology,[19] introducing mesopores into the zeolites,[20−22] or producing nano-zeolites.[23] The particle morphology can be tuned through addition of an organic amine modifier[24,25] or through using a custom structure-directing agent (SDA) to produce zeolite nano-

Received: October 5, 2021
Revised: January 15, 2022
Accepted: January 17, 2022
Published: January 25, 2022

https://doi.org/10.1021/acs.iecr.1c03979
Ind. Eng. Chem. Res. 2022, 61, 1977−1984

sheets.[26] Mesopores can be created through introducing a templating component into the synthesis. Each of these approaches is promising, but the methods also require the introduction of an additional component to produce the desired structure. Whereas many types of nano-zeolites can be produced, it would be advantageous to produce nano-zeolites through using only the core components required to produce the zeolites.

Nano-zeolite MFI can be produced through altering the synthesis conditions of MFI to favor the nucleation of particles over the growth of particles.[27−29] High rates of nucleation lead to limited residual precursors for additional growth, limiting the overall size that is produced. High rates of nucleation have been achieved using many different methods, including two-stage varying temperature synthesis[28] and decreasing the synthesis temperature.[13] Of these methods, previous work has demonstrated that Lewis acid nano-zeolites can be produced at low temperatures.[28,29] The low-temperature synthesis proceeded similarly with and without the inclusion of a tin precursor.[13] Indeed, dynamic light scattering (DLS) was used to monitor the growth of particles over time, demonstrating that the inclusion of tin did not strongly affect the growth rate or final particle size.

These promising results for the use of Lewis acid nano-zeolites require additional work to overcome challenges associated with limited tin incorporation into the material and the low yield of the nano-zeolites. Whereas the synthesis of tin-substituted MFI (Sn-MFI) using conventional methods (i.e., a temperature of 160 °C) results in greater than 80% tin incorporation efficiency (defined as the actual Sn wt %/theoretical Sn wt % added to the synthesis gel), the low-temperature method produced tin-substituted nano-zeolites with an MFI framework (nano-Sn-MFI) with less than 30% tin incorporation efficiency.[13] Although the amount of tin incorporated into the framework could be increased through adding more tin precursor to the synthesis gel,[13] it would be desirable to determine if synthetic conditions could be modified to increase the tin incorporation efficiency.

One potential modification would be to change the tin source. The most common tin source used for zeolite synthesis has been tin tetrachloride pentahydrate ($SnCl_4 \cdot 5H_2O$).[2,7,10,30,31] Interestingly, previous work[32] investigating tin-substituted zeolite beta (Sn-beta) used different tin sources, including tin (IV) acetate ($Sn(OAc)_4$), tetraethyl ammonium hexafluoro stannate, tin (IV) oxide,[32] and tin (IV) butoxide[26] to synthesize Sn zeolites. In comparing different tin sources used to produce Lewis acid zeolites, it was found that the tin source affected the observed catalytic activity for the conversion of 1,3-dihydroxyacetone to methyl lactate.[32] The highest activity was achieved using tin (IV) acetate. It would be beneficial to investigate how different tin sources would impact the resultant material properties, including tin incorporation efficiency.

In addition to the low tin incorporation efficiency, the other limitation for Lewis acid zeolite is that the low-temperature synthesis method produces a low yield of the catalytic material.[23] The synthesis of nano-MFI at lower temperatures results in a yield of ∼25%, whereas conventional Si-MFI materials have a yield of ∼60%. Interestingly, previous work has shown that the yield could be increased through reducing the concentration of SDA in the synthesis mixture for aluminosilicate MFI,[33] but it is unclear how the system would behave with the addition of a Lewis acid heteroatom such as tin.

Commonly, the SDA used to produce nano-MFI is tetra propyl ammonium hydroxide (TPAOH). The hydroxide ion concentration affects the solution alkalinity and the rate of crystal growth and dissolution. Since the observed crystal growth rate is determined by the difference between the rates of surface attachment and crystal dissolution, changing the amount of SDA will affect the observed growth rates and yield.[33] A minimum threshold concentration of TPAOH is required for the crystallization of MFI since using less than the threshold concentration of SDA/SiO_2 ratio of 0.2:1 will not produce a crystalline material because of insufficient SDA to guide the formation of MFI. Since the resultant materials are affected by each component included in the synthesis mixture, it is valuable to examine the effect of changing these different parameters (i.e., TPAOH concentration and tin source) on the resulting catalytic activity.

The reaction of interest is the alcohol ring opening (ARO) of epoxides, as shown in Scheme 1. Epoxides are versatile and

Scheme 1. Ring Opening of an Epoxide (a) with an Alcohol (b) to Produce Either a Terminal Ether (c) or a Secondary Ether (d)

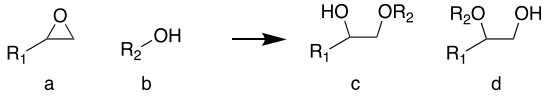

highly reactive chemical intermediates that can be ring-opened by a variety of nucleophiles (i.e., water,[8,9] amines,[34] and alcohols[10,13,35]) to produce different bifunctional products of industrial value.[36−39] Lewis acid zeolites have been determined to be highly active and more selective than similar Bronsted acid zeolites.[10] Our recent work synthesizing nano-zeolite Sn-MFI demonstrated that nano-zeolites could be used to overcome diffusion limitations when larger epoxides such as 1,2-epoxyhexane were ring-opened with methanol.[35] The catalysts would be promising if the synthesis methods could be tuned to produce higher yields of the nano-zeolites with greater amounts of tin incorporation.

The present work investigates how the synthesis method impacts the crystallization and the catalytic properties of Lewis acid nano-zeolites. Specifically, nano-Sn-MFI is synthesized using three different tin precursors using the conventional SDA TPAOH while using a synthesis temperature of 80 °C, which is known to produce nano-zeolites.[35] The particle size growth of all the tin-substituted particles is monitored using DLS. The synthesized materials are characterized using standard methods, including X-ray diffraction (XRD), nitrogen physisorption, elemental analysis, and diffuse reflectance UV−vis spectroscopy (DRUVS). The Lewis acid nano-MFI materials are tested for catalytic activity for the ARO of an epoxide as a model reaction. Overall, the work demonstrates how tuning the synthesis conditions can impact the tin incorporation efficiency and nano-zeolite yield and the corresponding effect on the catalytic activity of the material.

EXPERIMENTAL METHODS

Chemicals. All the chemicals are used as received without any further purification. The following chemicals are used: tetraethyl orthosilicate (TEOS; reagent grade, 98%, Acros Organics), TPAOH (40 wt % solution in water, EMD

https://doi.org/10.1021/acs.iecr.1c03979
Ind. Eng. Chem. Res. 2022, 61, 1977−1984

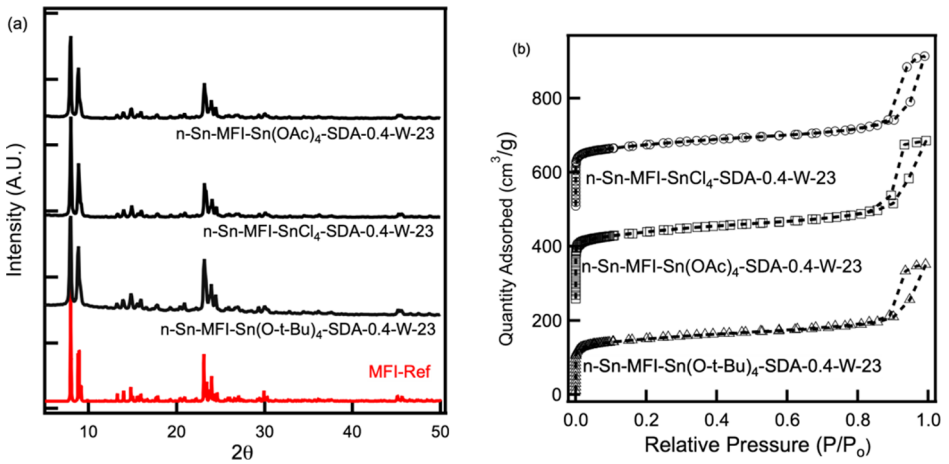

Figure 1. (a) XRD spectra for nano-MFI samples synthesized from different precursors. (b) Nitrogen physisorption isotherms of nano-Sn-MFI synthesized from different precursors. The data for $Sn(OAc)_4$ and $SnCl_4$ are offset for clarity by 250 and 500 cm^3/g, respectively.

Table 1. Properties of Nano-Sn-MFI Materials Synthesized from Different Precursors and Compositions

sample	surface area (m^2/g)[a]	micropore surface area (m^2/g)[b]	Sn (wt %)[c]	Sn incorporation efficiency (%)	synthesis yield (%)
n-Sn-MFI-$SnCl_4$-SDA-0.4-W-23	650	348	0.286	29	24
n-Sn-MFI-$Sn(OAc)_4$-SDA-0.4-W-23	700	370	0.368	38	25
n-Sn-MFI-$Sn(O\text{-}t\text{-}Bu)_4$-SDA-0.4-W-23	560	289	0.063	6	
n-Sn-MFI-$SnCl_4$-SDA-0.2-W-23	520	260	0.558	57	43
n-Sn-MFI-$Sn(OAc)_4$-SDA-0.2-W-23	520	268	0.513	52	40
n-Sn-MFI-$SnCl_4$-SDA-0.2-W-19	530	298	0.399	41	78
n-Sn-MFI-$Sn(OAc)_4$-SDA-0.2-W-19	540	288	0.440	45	72

[a]Based on nitrogen physisorption, BET method. [b]Based on nitrogen physisorption, t-plot method. [c]Based on elemental analysis.

Millipore), epichlorohydrin (ECH; 99%, BeanTown Chemical), 1,2-epoxyhexane (>96%, TCI), methanol (MeOH; HPLC grade, Fisher Chemical), diethylene glycol dibutyl ether (DGDE; >98%, TCI), tin (IV) acetate ($Sn(OAc)_4$, Sigma-Aldrich), tin (IV) tertiary butoxide ($Sn(O\text{-}t\text{-}Bu)_4$; ≥99.99% trace metals basis, Sigma-Aldrich), and tin (IV) chloride pentahydrate ($SnCl_4{\cdot}5H_2O$, 98%, Alfa Aesar). Deionized (DI) water is obtained from house supply.

Synthesis Procedure of Nano-Zeolite MFI. Nano-Sn-MFI is synthesized using a method similar to the synthesis method in previous literature.[13] Briefly, nano-Sn-MFI is synthesized by adding 5.2 g of TEOS and the tin precursor to the synthesis vessel. The ratio of Si/Sn used in the synthesis is 200:1, which corresponds to the mass included in Table S1. This SiO_2−SnO_2 synthesis gel is allowed to stir for 30 min. TPAOH (10.9 g; 20% wt aq; the 40 wt % solution is diluted to achieve the desired concentration) is added to this synthesis gel dropwise and allowed to stir for one more hour. To this solution, DI water (4.51 g) is added, and this synthesis gel is hydrolyzed for 24 h at room temperature while stirring. For the synthesis of nanosized MFI, the material is placed in an oven at a temperature of 80 °C. This reaction mixture is then allowed to crystallize for 5−10 days, depending on the time required for the materials to achieve a constant particle size as measured by DLS. After a fixed period of time, the material is removed from the oven, washed with water, and separated by centrifugation at 9000 rpm. These materials are dried in an oven overnight and calcined at 550 °C to remove the SDA. All characterization data are associated with the calcined materials. The synthesis yield is calculated based on the ratio of the mass of the freshly calcined material to the theoretical mass of SnO_2 and SiO_2 (produced from TEOS hydrolysis). The synthesis conditions are modified by changing the amount of water or SDA. The nano-zeolites produced using different syntheses are labeled according to the convention n-Sn-MFI-*X*-SDA-*Y*-W-*Z*, where *X* is the tin precursor, *Y* is the SDA/SiO_2 ratio, and *Z* is the H_2O/SiO_2 ratio. For example, the standard synthesis conditions use $SnCl_4$ as the tin precursor, and the material is named n-Sn-MFI-$SnCl_4$-SDA-0.4-W-23. The synthesis of pure silica n-Si-MFI is found in the Supporting Information (S1).

Materials Characterization and Catalytic Testing. The materials are characterized using several methods, including XRD, nitrogen physisorption, DLS, scanning electron microscopy (SEM), DRUVS, and elemental analysis. Since the analytical methods are the same as those in our previous work,[13] the details are included in the Supporting Information (S2). Similarly, the catalytic properties are evaluated using methods that we have reported previously, and the methods can be found in the Supporting Information (S3). This work focuses on the catalytic activity of the materials for the epoxide ring opening reaction of epichlorohydrin or 1,2-epoxyhexane with methanol.

RESULTS AND DISCUSSION

Synthesis and Characterization. The synthesis conditions are successful in producing nano-MFI using three different precursors (tin tetrachloride, tin tetra acetate, or tin tetra *t*-butoxide). For n-Sn-MFI made using tin chloride as a precursor, the material is separated using centrifugation and calcined at 550 °C. After calcination, the material is characterized using XRD and nitrogen physisorption. The XRD pattern of the material is consistent with the MFI

https://doi.org/10.1021/acs.iecr.1c03979
Ind. Eng. Chem. Res. 2022, 61, 1977−1984

structure, as shown in Figure 1a. The XRD data are used to calculate the relative crystallinity,[40] as shown in Table 1. Except for n-Sn-MFI-Sn(O-*t*-Bu)$_4$-SDA-0.4-W-23, the materials are highly crystalline with a relative crystallinity greater than 90%. Nitrogen physisorption on the materials reveals that the materials are porous with a high surface area and are crystalline by 6 days. The adsorption isotherm of the conventional material is type II, which is typical of nano-zeolites. The increase in micropore surface area for nano-zeolite relative to the conventional zeolite synthesis (e.g., 380 m^2/g)[13] is associated with the small crystal size and interparticle porosity. Indeed, a hysteresis loop is observed at high relative pressure values, reflecting the difference in pressure required to adsorb and desorb nitrogen. The small size of the nano-zeolites allows them to pack closely together, creating small voids between the particles where capillary condensation can occur. This condensation is commonly attributed to the presence of interparticle pores associated with particle aggregation.

Using the same synthesis method, n-Sn-MFI crystals are synthesized using tin acetate and tin butoxide precursors. Powder XRD patterns are consistent with the MFI structure, and nitrogen physisorption isotherms are used to calculate the surface area and micropore volume of nano-MFI samples. Details of the characterization are presented in the Table 1. In addition to the textural properties, the results in Table 1 include the elemental analysis results for Sn. It is observed that the weight percentage of tin in n-Sn-MFI-SnCl$_4$-SDA-0.4-W-23 is 0.286 wt %, which corresponds to a tin incorporation efficiency of 29%, which is consistent with our previous work.[13] Interestingly, the material made with the tin acetate precursor (n-Sn-MFI-Sn(OAc)$_4$-SDA-0.4-W-23) is found to have a higher weight percentage of 0.368%, but the material made with tin butoxide (n-Sn-MFI-Sn(O-*t*-Bu)$_4$-SDA-0.4-W-23) has a very low tin incorporation efficiency of 6%. The low tin incorporation efficiency for the tin butoxide precursor is undesirable, and no additional materials are synthesized using the tin butoxide precursor.

As each component of the synthesis gel can affect the crystallization process, it is important to investigate the particle growth kinetics of the materials. Whereas previous work has shown using XRD that the MFI structure is formed at all times, our work focuses on the synthesis and characterization of the materials after a steady-state particle size has been achieved.[41] The growth of the particles during synthesis is monitored by extracting samples at different times during crystallization and analyzing the samples using DLS to determine particle size as a function of time, as shown in Figure 2. Previous studies of DLS on n-Sn-MFI synthesized from tin chloride have shown particles with a size of around 90−100 nm and a crystallization time of 4 days.[13,27,28] At a temperature of 80 °C, the material growth continues over a period of approximately 4 days to achieve a steady-state particle size of 110−120 nm, which is summarized in Table 2 and is similar to the values reported in the literature.[13,27,28] The steady-state particle size varies little over time, suggesting that particle growth loses its driving force under these conditions. DLS on pure nano-Si-MFI (n-Si-MFI-SDA-0.4-W-23) particles is also done as a reference to see the change in the particle growth kinetics because of the inclusion of the tin precursor. From Figure 2, the crystallization in the presence of Sn proceeds at a similar rate as the pure silica material. The material growth follows a similar trend, and the inclusion of tin has a minimal impact on the growth rate of MFI crystals, but the final particle size of pure nano-Si-MFI is

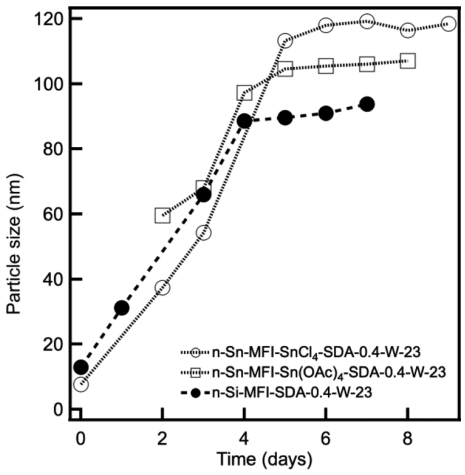

Figure 2. Comparison of particle size monitored using DLS for n-Si-MFI and n-Sn-MFI synthesized from tin chloride or tin acetate. The synthesis mixtures have an initial composition of 1 TEOS/0.4 TPAOH/23 H_2O/x Sn, where x is 0.005 for tin-containing syntheses and 0 for pure silica materials. The mixtures are hydrolyzed at room temperature for 24 h before the temperature of the mixture is increased to 80 °C (t = 0).

Table 2. Comparison of the Final Particle Size as Measured Using DLS and SEM of the nano-MFI Samples Synthesized Using Different Precursors and Different Compositions

sample	DLS particle size (nm)	SEM particle size (nm)
n-Si-MFI-SDA-0.4-W-23	90	70[a]
n-Sn-MFI-SnCl$_4$-SDA-0.4-W-23	115	100[a]
n-Sn-MFI-Sn(OAc)$_4$-SDA-0.4-W-23	105	-[b]
n-Sn-MFI-SnCl$_4$-SDA-0.2-W-23	170	160 ± 20
n-Sn-MFI-Sn(OAc)$_4$-SDA-0.2-W-23	170[c]	250 ± 30
n-Sn-MFI-SnCl$_4$-SDA-0.2-W-19	130	150 ± 10
n-Sn-MFI-Sn(OAc)$_4$-SDA-0.2-W-19	130	140 ± 10

[a]Reported previously.[13] [b]Not analyzed because of low tin incorporation efficiency. [c]Filtered using a 0.2 μm syringe filter before analysis.

slightly smaller than the particle size of n-Sn-MFI-SnCl$_4$-SDA-0.4-W-23, indicating slight differences in the growth process. The difference in size could be associated with tin species reducing the rate of nucleation, causing fewer particles to form, and leaving more silica species for growth. The additional growth species contribute to the increase in particle size. With the tin acetate precursor, the material (n-Sn-MFI-Sn(OAc)$_4$-SDA-0.4-W-23) grows similarly, reaching a final particle size of 100 nm. Overall, these results demonstrate that the tin precursor has a minor impact on the final particle size and growth kinetics. The particle size is also analyzed using SEM for the n-Sn-MFI material, as shown in Figure S3, with corresponding particle size distributions shown in Figure S4. From a series of images, the particle size for the different materials is determined through measuring the size of a range of particles. The comparison of the sizes calculated using DLS and SEM is given in Table 2. One discrepancy between SEM and DLS particle sizes could be noted for n-Sn-MFI-Sn(OAc)$_4$-SDA-0.2-W-23; where the particle size measured from SEM is over 200 nm, whereas the particle size from DLS is less than 200 nm. The discrepancy likely is the result of filtering the sample before DLS analysis. In general, the DLS

https://doi.org/10.1021/acs.iecr.1c03979
Ind. Eng. Chem. Res. 2022, 61, 1977−1984

analysis captures the approximate particle size achieved from the different material synthesis conditions.

Whereas changing the tin precursor has a moderate impact on increasing the heteroatom incorporation, changing the tin precursor had a minimal impact on the synthesis yield, as shown in Table 1. Indeed, the synthesis yield was around 25% for all nano-zeolites when using an SDA/SiO_2 ratio of 0.4 and a H_2O/SiO_2 ratio of 23. The yield remained constant even after an extended crystallization period of 20 days, as shown in Figure 3. This suggests that the composition of the zeolite

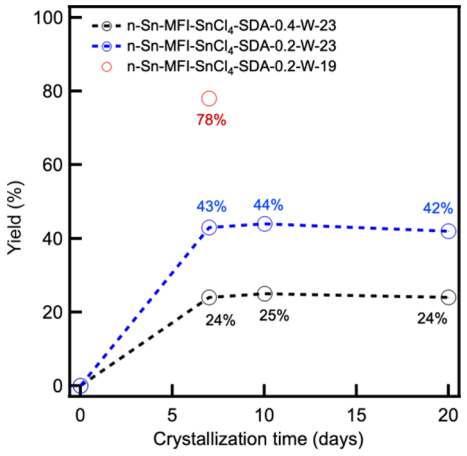

Figure 3. Comparison of the material yield over time for materials made using tin chloride with different amounts of SDA and water. The materials are crystallized at 80 °C.

synthesis mixture has achieved a steady state since no additional particles are formed, and the particle size remains constant. Overall, this suggests that the tin precursor counterion had a small impact on the rate of nucleation, resulting in a slight change in particle size, but the tin precursor did not affect yield.

As the tin precursor did not impact yield, it may be possible to use previous strategies to increase the yield of aluminosilicate nano-zeolite MFI by reducing the SDA concentration.[33] The synthesis gel composition is modified to be 1.0 TEOS/0.005 Sn/0.2 TPAOH/23 H_2O when using $SnCl_4$ as the tin source to produce n-Sn-MFI-SnCl4-SDA-0.2-W-23. The particle size over time is measured for this material synthesis gel, as shown in Figure 4. The particle size grows at a rate that is similar to earlier synthesis gel compositions. However, the growth continues beyond 120 nm up to a final particle size of 170 nm, as listed in Table 2. The final particle size is similar for the material synthesized with tin acetate (n-Sn-MFI-$Sn(OAc)_4$-SDA-0.2-W-23). The materials are characterized using standard techniques with the XRD data and nitrogen physisorption data shown in Figures S1 and S2. Combined, the XRD data and nitrogen physisorption data are consistent with the material being a highly crystalline MFI nano-zeolite.

Interestingly, the change in the SDA concentration impacts the tin incorporation efficiency and the yield of the Lewis acid nano-zeolite, as reported in Table 1. The reduced amount of SDA increases the yield from 25 to 43% or 40% when using the chloride or acetate precursor, respectively. The reduced amount of SDA also results in an increase in the tin incorporation efficiency for both precursors, increasing to 57 and 52% for the chloride and the acetate precursor,

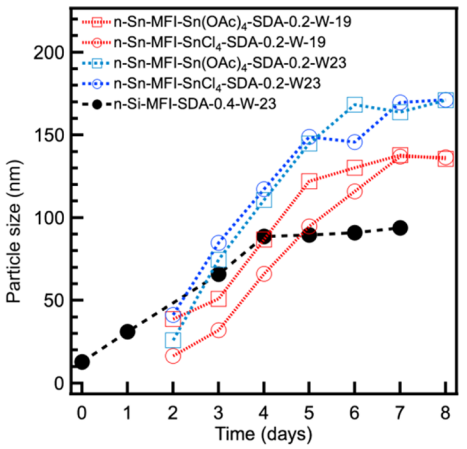

Figure 4. Comparison of particle size over time monitored using DLS for materials with a reduced TPAOH content. The synthesis gel composition is 1 TEOS/x Sn/0.2 TPAOH/y H_2O, where x is 0.005 for tin-containing syntheses and 0 for pure silica and y is either 19 or 23. The mixtures are hydrolyzed at room temperature for 24 h before the temperature of the mixture is increased to 80 °C (t = 0).

respectively (Table 1). These results demonstrate that the solution properties affect the resultant material synthesis with the likely source of the difference being the alkalinity of the synthesis gel.

The benefits of reducing the SDA concentration to increase need to be balanced with the potential limitation that the average particle size increased to 170 nm. It is possible that the synthesis composition can be further tuned to reduce the particle size. From the experimental data, reducing the concentration of the SDA causes the particles to grow to a greater extent than a higher SDA concentration. The nucleation rate can be increased through increasing the concentration of the reactants to increase the supersaturation. A subsequent synthesis is performed with a reduced SDA/SiO_2 ratio of 0.2 and a reduced H_2O/SiO_2 ratio of 19. As shown in Figure 4, the particle size changes over time are similar to the previous results. The final particle size is found to be 130 nm when using either the acetate or the chloride precursor, respectively. From XRD and nitrogen physisorption analysis, these materials are also found to be consistent with highly crystalline nano-MFI.

The modified synthesis conditions (SDA-0.2-W-19) impact the yield and the tin incorporation efficiency. Interestingly, the yield increases to 72% for the acetate precursor and 78% for the chloride precursor. These are substantial improvements over the initial yields of ∼25%. At the same time, the tin incorporation efficiencies are 41% (chloride precursor) and 45% (acetate precursor). The incorporation efficiencies are lower than the dilute conditions with limited SDA (SDA-0.2-W-23) but higher than the initial conditions (SDA-0.4-W-19). Based on these experiments, it is found that reducing the SDA/SiO_2 and H_2O/SiO_2 ratios can be an effective method to improve the yield and tin incorporation. These results can be used as a basis to guide additional experiments that would be beneficial to help optimize the conditions that produce the final material properties.

The potential formation of tin oxide is further investigated by analyzing the materials using DRUVS, as has been previously reported by us and others.[10,42] In the material, the Sn species can exist either in the zeolite framework or as extra-

https://doi.org/10.1021/acs.iecr.1c03979
Ind. Eng. Chem. Res. 2022, 61, 1977−1984

framework Sn species typically observed as SnO_2 species residing on the catalyst surface. A sample is prepared with extra-framework tin oxide by creating a physical mixture of tin oxide with pure n-Si-MFI-SDA-0.4-W-23 (labeled as n-Si-MFI) to produce 2% SnO_2@n-Si-MFI. The extra-framework SnO_2 species can give rise to a peak at 280 nm, as shown in Figure 5. For the materials produced using the conventional

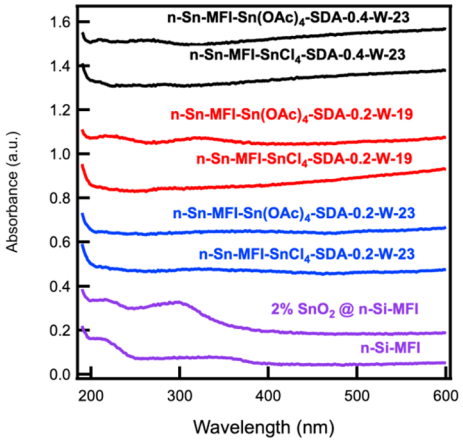

Figure 5. Comparison of the DRUVS spectra of n-Sn-MFI synthesized using tin chloride and tin acetate at different compositions along with physical mixtures of 2 wt % SnO_2@n-Si-MFI and n-Si-MFI. The materials are referenced to $MgSO_4$.

synthesis methods, the tail of a peak could be observed at 200 nm, which is commonly associated with framework tin species and does not contain a peak associated with SnO_2. For the material made using tin acetate (n-Sn-MFI-$Sn(OAc)_4$-SDA-0.4-W-23), a small peak appears around the 280 nm range. This may be associated with tin oxide, but additional evaluation is not performed since these synthesis conditions resulted in a low yield compared to other materials produced in this work. In general, the additional materials made using tin chloride or tin acetate with modified synthesis conditions did not have a peak in the DRUVS spectra that would be consistent with tin oxide.

Catalytic Testing. The nano-zeolite MFI materials are also tested for catalytic activity in the epoxide ring opening reaction with alcohol as a model reaction. Our previous work has examined how different epoxides are ring-opened, finding that the regioselectivity of the reaction for a specific epoxide is mainly influenced by the heteroatom.[10] Additionally, our previous work has also identified that the impact of diffusion limitations depends on the substrates, particle size,[13] and pore size.[35] Since the goal of this work is to increase the yield and tin incorporation of MFI nano-zeolites while maintaining a high-quality catalyst, the specific epoxides selected for the alcohol ring opening are epichlorohydrin or 1,2-epoxyhexane. Our combined previous work has demonstrated that the catalytic testing of epichlorohydrin is impacted by diffusion to a negligible extent when using the conditions outlined in the experimental methods (i.e., 0.4 M epoxide in alcohol with epoxide/Sn of 250:1 and a reaction temperature of 60 °C).[10,13,35] Therefore, this reaction can be used to compare the catalytic performance of the different material syntheses.

The materials are tested for catalytic activity by measuring the conversion of the epoxide over time, as shown in Figure 6. For the materials made using SDA-0.4-W-23, catalytic

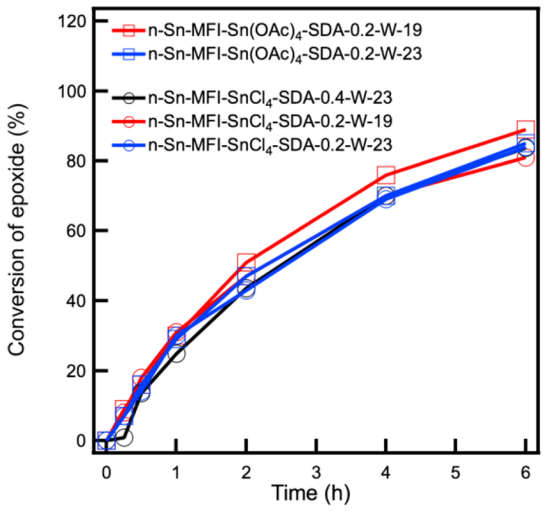

Figure 6. Comparison of conversion of epichlorohydrin with n-Sn-MFI catalysts synthesized from different precursors at different TPAOH concentrations. The reaction conditions include 63 μL of epichlorohydrin in 2 mL of methanol, 20 μL of DGDE (internal standard), a temperature of 60 °C, and a stirring speed of 600 rpm.

measurements are used to determine the activity for the material made with tin chloride (n-Sn-MFI-$SnCl_4$-SDA-0.4-W-23). The conversion is found to increase with time, consistent with first-order kinetics. These catalytic results are similar to those of our previous work that determined that the ring opening of epichlorohydrin with methanol is not diffusion-limited under the conditions tested. Additionally, it is determined that the selectivity for ring opening of epichlorohydrin with methanol is 97% for the terminal ether, consistent with the catalysts having Lewis acid catalytic sites.[10] For all catalysts, the selectivity is determined to be 97% and will not be discussed further.

Catalytic testing is also performed with the materials produced with a reduced TPAOH content, as shown in Figure 6. The catalytic testing with the n-Sn-MFI shows that the nanomaterial exhibits a higher conversion at all times during the reaction than the Sn-MFI materials reported previously.[13] Indeed, the n-Sn-MFI materials achieve a conversion of epichlorohydrin of >80% within 6 h. This is similar to the best performing n-Sn-MFI catalyst, indicating that the materials likely have a similar fraction of catalytic sites that are active. Overall, this demonstrates that it is possible to produce Lewis acid nano-zeolites with a modest tin incorporation efficiency (~41%) and a high yield (78%) that are highly active.

In addition to completing catalytic testing for the ring opening of epichlorohydrin with methanol, the materials synthesized using $SnCl_4$ are tested for catalytic activity for the ring opening of 1,2-epoxyhexane with methanol. Our previous work established that this reaction is affected by the particle size for n-Sn-MFI.[13] As shown in Figure 7, the conversion of the epoxide with either of the $SnCl_4$ materials increases rapidly initially. The activity for n-Sn-MFI-$SnCl_4$-SDA-0.2-W-23 is lower than that for n-Sn-MFI-$SnCl_4$-SDA-0.2-W-19. The difference can be attributed to the difference in particle size since n-Sn-MFI-$SnCl_4$-SDA-0.2-W-23 has larger crystals than n-Sn-MFI-$SnCl_4$-SDA-0.2-W-19. Overall, the resulting catalytic properties demonstrate the benefit of tuning the synthesis conditions to increase the yield and reduce the water content to decrease the particle size.

https://doi.org/10.1021/acs.iecr.1c03979
Ind. Eng. Chem. Res. 2022, 61, 1977−1984

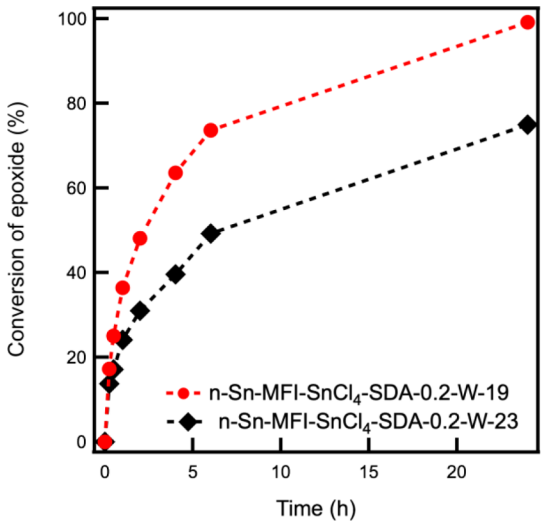

Figure 7. Comparison of conversion of 1,2-epoxyhexane with n-Sn-MFI catalysts synthesized with $SnCl_4$ at different TPAOH concentrations. The reaction conditions include 0.4 M 1,2-epoxyhexane in 2 mL of methanol, 20 μL of DGDE (internal standard), a temperature of 60 °C, and a stirring speed of 600 rpm.

SUMMARY

The synthesis of Lewis acid nano-zeolites with the MFI structure can be tuned to increase the yield and tin incorporation efficiency. The yield can be increased through reducing the SDA/SiO_2 ratio in the mixture to 0.2. Since decreasing the SDA/SiO_2 ratio reduces the supersaturation of the synthesis gel, the water content can be adjusted to maintain small particles. Combined, the low SDA/SiO_2 (0.2) and water/SiO_2 (19) ratios result in a yield of 78% of Lewis acid MFI nano-zeolites. At the lower SDA/SiO_2 of 0.2, the tin incorporation efficiency increases up to 40% or more. The resultant materials are highly active for the epoxide ring opening of epichlorohydrin with methanol, demonstrating the successful improvement of the synthetic procedure for Lewis acid MFI nano-zeolites.

ASSOCIATED CONTENT

Supporting Information

The Supporting Information is available free of charge at https://pubs.acs.org/doi/10.1021/acs.iecr.1c03979.

Details of materials characterization, catalytic testing, and characterization data (PDF)

AUTHOR INFORMATION

Corresponding Author

Nicholas A. Brunelli − *William G. Lowrie Department of Chemical and Biomolecular Engineering, The Ohio State University, Columbus, Ohio 43210, United States;* orcid.org/0000-0003-0712-8966; Email: brunelli.2@osu.edu

Authors

Medha Kasula − *William G. Lowrie Department of Chemical and Biomolecular Engineering, The Ohio State University, Columbus, Ohio 43210, United States*

Alexander P. Spanos − *William G. Lowrie Department of Chemical and Biomolecular Engineering, The Ohio State University, Columbus, Ohio 43210, United States*

Leah Ford − *William G. Lowrie Department of Chemical and Biomolecular Engineering, The Ohio State University, Columbus, Ohio 43210, United States*

Complete contact information is available at: https://pubs.acs.org/10.1021/acs.iecr.1c03979

Notes

The authors declare no competing financial interest.

ACKNOWLEDGMENTS

This work was supported by the National Science Foundation (NSF Career 1653587) and the Ohio State University Institute for Materials Research (OSU IMR FG0211) for their financial support.

REFERENCES

(1) Corma, A.; Nemeth, L. T.; Renz, M.; Valencia Valencia, S.; Valencia, S. Sn-Zeolite Beta as a Heterogeneous Chemoselective Catalyst for Baeyer-Villiger Oxidations. *Nature* **2001**, *412*, 423−425.

(2) Moliner, M.; Roman-Leshkov, Y.; Davis, M. E. Tin-Containing Zeolites Are Highly Active Catalysts for the Isomerization of Glucose in Water. *Proc. Natl. Acad. Sci.* **2010**, *107*, 6164−6168.

(3) Gunther, W. R.; Wang, Y.; Ji, Y.; Michaelis, V. K.; Hunt, S. T.; Griffin, R. G.; Román-Leshkov, Y. Sn-Beta Zeolites with Borate Salts Catalyse the Epimerization of Carbohydrates via an Intramolecular Carbon Shift. *Nat. Commun.* **2012**, *3*, 1109.

(4) Lewis, J. D.; Van de Vyver, S.; Román-Leshkov, Y.; Van de Vyver, S.; Román-Leshkov, Y. Acid-Base Pairs in Lewis Acidic Zeolites Promote Direct Aldol Reactions by Soft Enolization. *Angew. Chem., Int. Ed.* **2015**, *54*, 9835−9838.

(5) Bates, J. S.; Gounder, R. Influence of Confining Environment Polarity on Ethanol Dehydration Catalysis by Lewis Acid Zeolites. *J. Catal.* **2018**, *365*, 213−226.

(6) Pacheco, J. J.; Davis, M. E. Synthesis of Terephthalic Acid via Diels-Alder Reactions with Ethylene and Oxidized Variants of 5-Hydroxymethylfurfural. *Proc. Natl. Acad. Sci. U.S.A.* **2014**, *111*, 8363−8367.

(7) Corma, A.; Domine, M. E.; Nemeth, L.; Valencia, S. Al-Free Sn-Beta Zeolite as a Catalyst for the Selective Reduction of Carbonyl Compounds (Meerwein-Ponndorf-Verley Reaction). *J. Am. Chem. Soc.* **2002**, *124*, 3194−3195.

(8) Tang, B.; Dai, W.; Wu, G.; Guan, N.; Li, L.; Hunger, M. Improved Postsynthesis Strategy to Sn-Beta Zeolites as Lewis Acid Catalysts for the Ring-Opening Hydration of Epoxides. *ACS Catal.* **2014**, *4*, 2801−2810.

(9) Dai, W.; Wang, C.; Tang, B.; Wu, G.; Guan, N.; Xie, Z.; Hunger, M.; Li, L. Lewis Acid Catalysis Confined in Zeolite Cages as a Strategy for Sustainable Heterogeneous Hydration of Epoxides. *ACS Catal.* **2016**, *6*, 2955.

(10) Deshpande, N.; Parulkar, A.; Joshi, R.; Diep, B.; Kulkarni, A.; Brunelli, N. A. Epoxide Ring Opening with Alcohols Using Heterogeneous Lewis Acid Catalysts: Regioselectivity and Mechanism. *J. Catal.* **2019**, *370*, 46−54.

(11) Copéret, C.; Chabanas, M.; Saint-Arroman, R. P.; Basset, J.-M. Homogeneous and Heterogeneous Catalysis: Bridging the Gap through Surface Organometallic Chemistry. *Angew. Chem., Int. Ed.* **2003**, *42*, 156−181.

(12) Mastropietro, T. F.; Drioli, E.; Poerio, T. Low Temperature Synthesis of Nanosized NaY Zeolite Crystals from Organic-Free Gel by Using Supported Seeds. *RSC Adv.* **2014**, *4*, 21951−21957.

(13) Parulkar, A.; Joshi, R.; Deshpande, N.; Brunelli, N. A. Synthesis and Catalytic Testing of Lewis Acidic Nano-MFI Zeolites for the Epoxide Ring Opening Reaction with Alcohol. *Appl. Catal., A* **2018**, *566*, 25−32.

(14) Xu, C.; Lu, X.; Wang, Z. Effects of Sodium Ions on the Separation Performance of Pure-Silica MFI Zeolite Membranes. *J. Membr. Sci.* **2017**, *524*, 124−131.

(15) Zhang, J.; Li, X.; Liu, J.; Wang, C. A Comparative Study of MFI Zeolite Derived from Different Silica Sources: Synthesis, Characterization and Catalytic Performance. *Catalysts* **2018**, *9*, 13.
(16) Musselwhite, N.; Na, K.; Sabyrov, K.; Alayoglu, S.; Somorjai, G. A. Mesoporous Aluminosilicate Catalysts for the Selective Isomerization of N-Hexane: The Roles of Surface Acidity and Platinum Metal. *J. Am. Chem. Soc.* **2015**, *137*, 10231−10237.
(17) Moliner, M. State of the Art of Lewis Acid-Containing Zeolites: Lessons from Fine Chemistry to New Biomass Transformation Processes. *Dalton Trans.* **2014**, *43*, 4197−4208.
(18) Corma, A.; García, H. Lewis Acids: From Conventional Homogeneous to Green Homogeneous and Heterogeneous Catalysis. *Chem. Rev.* **2003**, *103*, 4307−4366.
(19) Lupulescu, A. I.; Qin, W.; Rimer, J. D. Tuning Zeolite Precursor Interactions by Switching the Valence of Polyamine Modifiers. *Langmuir* **2016**, *32*, 11888−11898.
(20) Christensen, C.; Johannsen, K.; Törnqvist, E.; Schmidt, I.; Topsøe, H.; Christensen, C. Mesoporous Zeolite Single Crystal Catalysts: Diffusion and Catalysis in Hierarchical Zeolites. *Catal. Today* **2007**, *128*, 117−122.
(21) Groen, J. C.; Peffer, L. A. A.; Moulijn, J. A.; Pérez-Ramírez, J. On the Introduction of Intracrystalline Mesoporosity in Zeolites upon Desilication in Alkaline Medium. *Microporous Mesoporous Mater.* **2004**, *69*, 29−34.
(22) Egeblad, K.; Christensen, C. H.; Kustova, M.; Christensen, C. H. Templating Mesoporous Zeolites. *Chemistry of Materials*; American Chemical Society, 2008; Vol. *20*, pp 946−960.
(23) Tosheva, L.; Valtchev, V. P. Nanozeolites: Synthesis, Crystallization Mechanism, and Applications. *Chem. Mater.* **2005**, *17*, 2494−2513.
(24) Lupulescu, A. I.; Rimer, J. D. Tailoring Silicalite-1 Crystal Morphology with Molecular Modifiers. *Angew. Chem., Int. Ed.* **2012**, *51*, 3345−3349.
(25) Li, R.; Smolyakova, A.; Maayan, G.; Rimer, J. D. Designed Peptoids as Tunable Modifiers of Zeolite Crystallization. *Chem. Mater.* **2017**, *29*, 9536−9546.
(26) Luo, H. Y.; Bui, L.; Gunther, W. R.; Min, E.; Román-Leshkov, Y. Synthesis and Catalytic Activity of Sn-MFI Nanosheets for the Baeyer − Villiger Oxidation of Cyclic Ketones. *ACS Catal.* **2012**, *2*, 2695−2699.
(27) Aguado, J.; Serrano, D. P.; Escola, J. M.; Rodríguez, J. M. Low Temperature Synthesis and Properties of ZSM-5 Aggregates Formed by Ultra-Small Nanocrystals. *Microporous Mesoporous Mater.* **2004**, *75*, 41−49.
(28) Li, Q.; Creaser, D.; Sterte, J. The Nucleation Period for TPA-Silicalite-1 Crystallization Determined by a Two-Stage Varying-Temperature Synthesis. *Microporous Mesoporous Mater.* **1999**, *31*, 141−150.
(29) Li, Q.; Mihailova, B.; Creaser, D.; Sterte, J. Aging Effects on the Nucleation and Crystallization Kinetics of Colloidal TPA-Silicalite-1. *Microporous Mesoporous Mater.* **2001**, *43*, 51−59.
(30) Valencia Valencia, S.; Corma, A. Stannosilicate Molecular Sieves. U.S. Patent 6,306,364 B1, 2001.
(31) Harris, J. W.; Bates, J. S.; Bukowski, B. C.; Greeley, J.; Gounder, R. Opportunities in Catalysis over Metal-Zeotypes Enabled by Descriptions of Active Centers Beyond Their Binding Site. *ACS Catal.* **2020**, *10*, 9476−9495.
(32) Tolborg, S.; Katerinopoulou, A.; Falcone, D. D.; Sádaba, I.; Osmundsen, C. M.; Davis, R. J.; Taarning, E.; Fristrup, P.; Holm, M. S.; Sádaba, I.; Osmundsen, C. M.; Davis, R. J.; Taarning, E.; Fristrup, P.; Holm, M. S. Incorporation of Tin Affects Crystallization, Morphology, and Crystal Composition of Sn-Beta. *J. Mater. Chem. A* **2014**, *2*, 20252−20262.
(33) Persson, A. E.; Schoeman, B. J.; Sterte, J.; Otterstedt, J.-E. Synthesis of Stable Suspensions of Discrete Colloidal Zeolite (Na, TPA)ZSM-5 Crystals. *Zeolites* **1995**, *15*, 611−619.
(34) Tang, B.; Dai, W.; Sun, X.; Wu, G.; Guan, N.; Hunger, M.; Li, L. Mesoporous Zr-Beta Zeolites Prepared by a Post-Synthetic Strategy as a Robust Lewis Acid Catalyst for the Ring-Opening Aminolysis of Epoxides. *Green Chem.* **2015**, *17*, 1744−1755.
(35) Parulkar, A.; Spanos, A. P.; Deshpande, N.; Brunelli, N. A. Synthesis and Catalytic Testing of Lewis Acidic Nano Zeolite Beta for Epoxide Ring Opening with Alcohols. *Appl. Catal., A* **2019**, *577*, 28−34.
(36) Williams, D. B.; Lawton, M.; Lawton, M. Aluminium Triflate: A Remarkable Lewis Acid Catalyst for the Ring Opening of Epoxides by Alcohols. *Org. Biomol. Chem.* **2005**, *3*, 3269−3272.
(37) Zhao, P.-Q.; Xu, L.-W.; Xia, C.-G. Transition Metal-Based Lewis Acid Catalyzed Ring Opening of Epoxides Using Amines Under Solvent-Free Conditions. *Synlett* **2004**, *5*, 0846−0850.
(38) Liu, Y.; Klet, R. C.; Hupp, J. T.; Farha, O. Probing the Correlations between the Defects in Metal-Organic Frameworks and Their Catalytic Activity by an Epoxide Ring-Opening Reaction. *Chem. Commun.* **2016**, *52*, 7806−7809.
(39) Prestat, G.; Baylon, C.; Heck, M.-P.; Mioskowski, C. Lewis Acid-Catalyzed Regiospecific Opening of Vinyl Epoxides by Alcohols. *Tetrahedron Lett.* **2000**, *41*, 3829−3831.
(40) Kalita, B.; Talukdar, A. K. An Efficient Synthesis of Nanocrystalline MFI Zeolite Using Different Silica Sources: A Green Approach. *Mater. Res. Bull.* **2009**, *44*, 254−258.
(41) Li, Q.; Mihailova, B.; Creaser, D.; Sterte, J. The Nucleation Period for Crystallization of Colloidal TPA-Silicalite-1 with Varying Silica Source. *Microporous Mesoporous Mater.* **2000**, *40*, 53−62.
(42) Bermejo-Deval, R.; Gounder, R.; Davis, M. E. Framework and Extraframework Tin Sites in Zeolite Beta React Glucose Differently. *ACS Catal.* **2012**, *2*, 2705−2713.

https://doi.org/10.1021/acs.iecr.1c03979
Ind. Eng. Chem. Res. 2022, 61, 1977−1984